Published in final edited form as:
Biochem J. 2014 May 1; 459(3): 539–550. doi:10.1042/BJ20131681.

The Upstream Conserved Regions (UCRs) Mediate Homo- and Hetero-oligomerization of Type 4 Cyclic Nucleotide Phosphodiesterases (PDE4s)

Moses Xie[1], **Brigitte Blackman**, **Colleen Scheitrum**, **Delphine Mika**, **Elise Blanchard**, **Tao Lei**, **Marco Conti**, and **Wito Richter**[2]
Department of Obstetrics, Gynecology and Reproductive Sciences, University of California San Francisco, San Francisco, CA 94143, U.S.A

Abstract

Type 4 cyclic nucleotide phosphodiesterases (PDE4s) are divided into long and short forms by the presence or absence of conserved N-terminal domains termed upstream conserved regions (UCRs). We have shown previously that PDE4D2, a short variant, is a monomer, whereas PDE4D3, a long variant, is a dimer. Here, we have determined the apparent molecular weights of various long and short PDE4 variants by size exclusion chromatography and sucrose density gradient centrifugation. Our results indicate that dimerization is a conserved property of all long PDE4 forms, whereas short forms are monomers. Dimerization is mediated by the UCR domains. Given their high sequence conservation, the UCR domains mediate not only homo-oligomerization, but also hetero-oligomerization of distinct PDE4 long forms as detected by co-immunoprecipitation assays and FRET microscopy. Endogenous PDE4 hetero-oligomers are in low abundance, however, compared to homo-dimers revealing the presence of mechanisms that predispose PDE4s towards homo-oligomerization. Oligomerization is a prerequisite for regulatory properties of PDE4 long forms, such as their PKA-dependent activation, but is not necessary for PDE4 protein/protein interactions. As a result, individual PDE4 protomers may independently mediate protein/protein interactions, providing a mechanism whereby PDE4s contribute to the assembly of macromolecular signaling complexes.

Keywords

cAMP; phosphodiesterase; dimer; oligomerization; PDE4

INTRODUCTION

The mammalian cyclic nucleotide phosphodiesterases (PDEs), the enzymes that hydrolyze and inactivate the second messengers cAMP and cGMP, are encoded by 21 genes. They are grouped into 11 PDE families based on their kinetic and pharmacologic properties, substrate specificity and sequence homology [1]. The PDE4 family is the largest of the PDE families, comprising four genes, *PDE4A* to *PDE4D* [2]. PDE4 proteins are distinguished from other

[2]To whom correspondence should be addressed: richterw@obgyn.ucsf.edu.
[1]current address: Department of Neuroscience, Baylor College of Medicine, Houston, TX

PDEs by their high selectivity for cAMP over cGMP as substrate and their sensitivity to inhibition by the prototypal PDE4 inhibitor rolipram.

Each of the PDE4 genes is expressed as multiple variants *via* alternative splicing and use of alternate promoters/transcription start sites. To date, at least 25 unique PDE4 variants have been identified. These can be divided into long and short forms by the presence or absence of two highly conserved N-terminal domains termed upstream conserved regions 1 and 2 (UCR1 and UCR2) (Figure 1A) [2]. Long forms contain the complete set of UCR1 and UCR2, whereas short forms lack UCR1, but retain the entire, or at least a portion of UCR2. The presence or absence of the UCR domains determines critical functional differences between long and short forms. UCR1 harbors a PKA consensus site, and phosphorylation at this site mediates activation of PDE4 long forms [3, 4], thereby desensitizing cAMP signaling [5]. UCR1 also harbors a binding site for phosphatidic acid, which acts as an allosteric activator of long PDE4s [6, 7]. In addition, long and short forms respond differently to post-translation modifications that are conserved among them. PDE4B, PDE4C and PDE4D variants, for example, share a consensus site for phosphorylation by the extracellular signal-regulated kinase 2 (ERK2) at their C-terminus. Phosphorylation at this site induces inhibition of long forms, whereas short variants are either activated or do not respond with changes in activity [8, 9].

The extreme N-termini of PDE4s are often encoded by variant-specific first exons and are thus unique to individual PDE4 variants. These sequences often mediate protein/protein or protein/lipid interactions that serve to target the respective variant to specific subcellular compartments and/or signaling complexes [2, 10]. As a result, individual PDE4 variants control distinct subcellular pools of cAMP signaling and exert unique and non-overlapping physiologic and pathophysiologic functions.

We have shown previously that the short form PDE4D2 behaves as a monomer, whereas the long variant PDE4D3 forms dimers [11]. Two helices, located in the C-terminal half of UCR1 (UCR1C) and the N-terminal half of UCR2 (UCR2N), respectively, were identified as critical for PDE4D3 dimerization [11, 12]. Dimerization is critical for PDE4D3 function as ablation of dimerization eliminates activation of the enzyme by PKA phosphorylation and/or phosphatidic acid binding [12]. In addition, the variance in their quaternary structures is also responsible for differences in inhibitor sensitivity between PDE4D3 and PDE4D2. Here, we investigated whether dimerization is a conserved property that distinguishes PDE4 long and short forms, whether the UCR domains are responsible for dimerization, and if so, whether these highly conserved regions might also mediate hetero-oligomerization of PDE4s.

EXPERIMENTAL

Design of Expression Vectors

The following PDE4 expression constructs have been described previously: plasmids encoding rat PDE4D1-PDE4D6 [13]; plasmids encoding human PDE4D2 and PDE4D3 C-terminally tagged with either Myc- or V5-tags [11]; plasmids encoding human PDE4A4 and human PDE4B1 [14]. A construct encoding human PDE4A1 was generated by cloning the

open reading frame of this PDE4 variant in the pCMV5 vector. The construct 4Ashort was generated by subcloning the nucleotide sequence encoding amino acids 257-886 of HSPDE4A4 (NP_001104777.1) into the pCMV5 vector. The construct 4A4ΔUCR1C was generated by deletion mutagenesis and encodes a HSPDE4A4 lacking amino acids 181 to 200. Chimeras encoding the PDE4 UCR regions fused to a C-terminal GFP or RFP were generated by subcloning sequences encoding amino acids 134-296 of HSPDE4A4 or 107-206 of HSPDE4D3 into vectors pEGFP-N1 (Clontech, Mountain View, CA) and a vector expressing mRFP [15], which was kindly provided by Dr. R.Y. Tsien (University of California San Diego), respectively. Sequences encoding amino acids 1-225 of HSPDE4D3 were cloned in the vector pcDNA3.1-V5/His (Invitrogen/Life Technologies, Grand Island, NY) to generate the 4D3NT-V5 construct. For bacterial expression of a chimera of the SH3-binding domain of the tyrosine protein kinase Lyn with glutathione S-transferase (GST), the nucleotide sequence encoding amino acids 61 to 126 of human Lyn (NP_002341.1) was cloned into the pGEX-5x-3 vector (Pharmacia/GE Healthcare, Piscataway, NJ).

Cell Culture

COS7 and Hek293 cells were grown in Dulbecco's Modified Eagle Medium (DMEM) supplemented with 10 % fetal calf serum, 30 μg/ml penicillin and 100 μg/ml streptomycin and were cultured at 37°C under a 5% CO_2 atmosphere. For expression of recombinant protein, cells were transfected with recombinant vector DNA using Effectene (Invitrogen/Life Technologies) or Lipofectamine 2000 (FRET experiments; Invitrogen/Life Technologies), or infected with adenoviruses at an MOI of 100. GST and GST-fusion proteins were expressed in BL21(DE3)-*E. coli* cells transformed with pGEX-5x-3 vectors and were purified using glutathion-Sepharose (Pharmacia/GE Healthcare).

HPLC Size Exclusion Chromatography

Gel filtration experiments were performed as described previously [11, 16]. In brief, cells were harvested in buffer containing 10 mM sodium acetate (pH 6.5), 150 mM NaCl, 1 mM EDTA, 0.2 mM EGTA, 1.34 mM β-mercaptoethanol, 10 mM NaF, 20 % ethylene glycol, 1 mM AEBSF and a protease inhibitor mix from Roche Diagnostics (Indianapolis, IN). The cell homogenates were centrifuged first at 14,000 × *g* for 20 min followed by a 30 min centrifugation at 100,000 × *g*, and 500 μl of the high speed supernatant were then applied on a TSK-3000 analytical gel filtration column (Tosoh Bioscience LLC, Montgomeryville, PA). The samples were eluted with buffer containing 10 mM sodium acetate (pH 6.5), 150 mM NaCl, 1 mM EDTA, 0.2 mM EGTA, 1.34 mM β-mercaptoethanol, 10 mM NaF, and 20 % ethylene glycol at a flow rate of 0.5 ml/min. Fractions of 500 μl were collected and assayed for PDE activity. Molecular weight markers assayed under the same conditions were bovine thyroglobulin (670 kDa; 85 Å), horse ferritin (440 kDa; 61 Å), bovine gamma globulin (158 kDa), rabbit aldolase (158 kDa; 48.1 Å), bovine serum albumin (monomer = 67 kDa; 35.5 Å), chicken ovalbumin (44 kDa; 30.5 Å), horse myoglobin (17 kDa), and cobalamin (1.35 kDa).

Density gradient centrifugation

Density gradients from 5 to 33 % sucrose in 50 mM Tris-HCl (pH 8.0), 150 mM NaCl, 1 mM EDTA, 0.2 mM EGTA, 10 mM NaF and 1.34 mM β-mercaptoethanol were prepared in 14x89-mm centrifugation tubes (Beckman Coulter Inc., Brea, CA) using the Jule gradient former (Jule Inc., New Haven, CT) as previously described [11, 16]. The gradients were stored overnight at 4°C before they were loaded with 100 μl of the soluble cell extracts (100,000 × *g* supernatant) or marker proteins and centrifuged for 24 h at 36,000 rpm in a Beckman SW41 rotor (Beckman Coulter Inc., Brea, CA). Fractions of ~220 μl were then collected starting from the bottom of the tube using a peristaltic pump and analyzed for PDE activity or protein concentration (molecular weight markers). The following proteins were used as molecular weight markers: bovine thyroglobulin (670 kDa; 19 S), bovine liver catalase (250 kDa; 11.3 S), rabbit aldolase (158 kDa; 7.3 S), bovine serum albumin (67 kDa; 4.6 S), and chicken ovalbumin (44 kDa; 3.5 S).

Calculation of Molecular Weights

The molecular weights of PDE4 constructs were calculated by the method of Siegel and Monty [17] as described previously [16] using the Stokes radii and sedimentation coefficients obtained from gel filtration and density gradient centrifugation, respectively, using the equation:

$$M=(S_w \cdot N_A \cdot 6 \cdot \pi \cdot \eta \cdot R_s)/(1-v_2 \cdot \rho)$$

or simplified

$$M=S_w \cdot R_s \cdot 4.2$$

where S_w = sedimentation coefficient in Svedberg units; N_A = Avogadro's constant ($6.022 \cdot 10^{23}$ mol^{-1}); η = viscosity of medium (0.01 $g \cdot cm^{-1} \cdot s^{-1}$); R_s = Stokes radius in nm (10 Å = 1 nm); v_2 = partial specific volume of a protein (0.73 $cm^3 \cdot g^{-1}$); and ρ = density of medium (1 $g \cdot cm^{-3}$).

Antibodies and Immunoprecipitation (IP)

For IP, cells were routinely harvested in 50 mM Tris-HCl (pH 8.0) containing 150 mM NaCl, 1 mM EDTA, 0.2 mM EGTA, 10 mM NaF, 10 mM sodium pyrophosphate, 1.34 mM β-mercaptoethanol, 1 μM microcystin and a protease inhibitor cocktail from Roche Diagnostics (Indianapolis, IN). IP was then performed as previously described [11]. The following antibodies were used in this study: α-V5 and α-Myc antibodies were from Invitrogen/Life Technologies and Roche Diagnostics, respectively. The PDE4A antibody AC55 [18], the PDE4B antibody K118 [18], the PDE4D antibody M3S1 [18] and the PAN-PDE4 antibody K116 [12] have been described previously. A mouse monoclonal antibody against PDE4D used for Western blotting was a gift from Icos Corporation (Bothell, WA).

PDE Assay

PDE activity was measured as described previously [11]. In brief, samples were assayed in a reaction mixture of 200 μl containing 40 mM Tris-HCl (pH 8.0), 1 mM $MgCl_2$, 1.34 mM β-mercaptoethanol, 1 μM cAMP, 0.75 mg/ml bovine serum albumin and 0.1 μCi [^{3}H]cAMP

for 10 min at 33°C followed by heat inactivation in a boiling water bath for 1 min. The PDE reaction product 5′-AMP was then hydrolyzed by incubation of the assay mixture with 50 μg *Crotalus atrox* snake venom for 20 min at 33°C and the resulting adenosine was afterwards separated by anion exchange chromatography on 1 ml of AG1-X8 resin and quantitated by scintillation counting.

PKA Phosphorylation Assay

For *in vitro* phosphorylation experiments, cytosolic supernatants of recombinant PDE constructs expressed in COS7 cells were incubated for 10 min at 30°C in a reaction mixture containing 20 mM $MgCl_2$, 200 μM ATP, 1 μM microcystin, and 1.0 U PKA catalytic subunit (Promega, Madison, WI). Samples were then assayed for PDE activity.

Fluorescence Microscopy and FRET Measurements

COS7 cells, grown on 25 mm glass coverslips (Fisher Scientific, Pittsburgh, PA) coated with Poly-D-Lysine (Sigma-Aldrich, St. Louis, MO), were transfected with plasmids encoding fluorescent protein-PDE chimeras using Lipofectamine 2000 (Invitrogen). Microscopy was performed after overnight culture in serum-free DMEM. The coverslips were placed in a modified Sykes-Moore Chamber and kept in 300 μl of phenol red-free DMEM containing 2 mM HEPES at 37°C. Images were acquired using a Nikon TE2000 inverted fluorescence microscope using a 100x epifluorescence objective and a xenon light source (Lambda LS, Sutter Instrument Company, Novato, CA). GFP (Donor) fluorescence was viewed by exciting at 480–495 nm and measuring emission at 500–530 nm. RFP (Acceptor) fluorescence was viewed by exciting at 500–560 nm and measuring emission at 580–630 nm. FRET was viewed by exciting at 480–495 nm (Donor excitation) and measuring fluorescence at 580–630 nm (Acceptor emission). Background and bleedthrough were subtracted from FRET images pixel by pixel to obtain corrected FRET images using MetaMorph software (Molecular Devices, Downingtown, PA).

RESULTS

Short PDE4 Variants are Monomers, Whereas Long Variants are Dimers

To resolve whether oligomerization is a conserved property of long PDE4 forms, but not short forms, we determined the apparent molecular weights of several PDE4A and PDE4D variants (Figure 1A) by size exclusion chromatography and density gradient centrifugation. As shown in Figure 1B/C, the short PDE4D variants PDE4D1, PDE4D2 and PDE4D6 eluted in similar fractions from gel filtration columns (Stokes radii of 49–51 Å) (Figure 1B) and showed a similar migration in sucrose density gradients (Sedimentation coefficients of 3.3 to 3.7 S) (Figure 1C). The only short form expressed from the PDE4A gene, PDE4A1, binds to lipids *via* its variant-specific N-terminus and is largely recovered in the membrane fraction of cell lysates [19]. After solubilization of the enzyme from the membrane fraction using 0.2% Triton, a major portion of PDE4A1 activity still eluted in the void volume of gel filtration columns, presumably due to interactions with lipids (Supplementary Figure S1) and/or formation of micelles. However, a minor portion of PDE4A1 eluted in similar fractions as the short PDE4D variants. In addition, the construct PDE4A-short, which encodes a PDE4A1 lacking the N-terminal membrane-targeting domain, behaved similar to

the short PDE4D variants in both gel filtration and density gradients (Figure 1B/C). The theoretical molecular weights of short PDE4s determined from their amino acid composition range from 58 to 70 kDa and the molecular weights calculated from their Stokes radii and sedimentation coefficients as described under *Experimental*, range from 68 to 79 kDa, suggesting that PDE4 short forms are monomers.

Next, we determined the apparent molecular weights of several long PDE4 variants. Long PDE4D variants PDE4D3, PDE4D4 and PDE4D5 as well as the PDE4A long form PDE4A4, all eluted in similar fractions from gel filtration columns (Stokes radii of 61–65 Å) (Figure 1D) and showed similar migration in sucrose density gradients (Sedimentation coefficients of 6.1 to 6.4 S) (Figure 1E). The theoretical molecular weights of PDE4 long forms range from 76 to 98 kDa, whereas their apparent molecular weights calculated from Stokes radii and sedimentation coefficients range from 156 to 175 kDa, suggesting that PDE4 long forms are dimers. Taken together, our data suggest that dimerization is a property conserved among PDE4 long forms, whereas short variants are monomers.

The UCR1C domain is critical for dimerization of long PDE4s

We previously identified a region encompassing the C-terminal half of UCR1 (UCR1C) and the N-terminal half of UCR2 (UCR2N) as critical for dimerization of PDE4D3 [11, 12]. To test whether dimerization of other PDE4 long forms is mediated by the same domains, a PDE4A4 construct lacking 20 amino acid residues within UCR1C, 4A4ΔUCR1, was generated (Figure 2A). Similar to findings with PDE4D3, this nested deletion within UCR1C disrupts dimerization of PDE4A4 as detected by size exclusion chromatography and sucrose density gradient centrifugation (Figure 2B/C). The theoretical molecular weights for full-length 4A4 and 4A4ΔUCR1C are 98 and 96 kDa, whereas their molecular weights calculated from stokes radii and sedimentation coefficients are 175 and 79 kDa, respectively, suggesting that 4A4 is a dimer, whereas 4A4ΔUCR1C is a monomer. This indicates that the presence of UCR1 is a general requirement for dimerization of long PDE4s. Similar to findings with PDE4D3, ablation of dimerization by nested deletion of UCR1C ablates the PKA-dependent activation of PDE4A4 (Figure 2D).

Detection of PDE4 hetero-oligomers by co-immunoprecipitation of recombinant PDE4 variants

The finding that long PDE4 variants dimerize *via* the UCR domains begs the question of whether these highly conserved domains may also mediate hetero-oligomerization between distinct PDE4 long forms. To test this idea, various PDE4D variants were expressed in COS7 cells either alone or co-expressed with 4D3NT-V5, a construct encoding the N-terminal domain of PDE4D3 including the UCR domains, fused to a V5-tag. After cell harvest, 4D3NT-V5 was immunoprecipitated and the IP pellet was probed for the presence of the full length PDE4D variants. As shown in Figure 3A, long variants, including PDE4D3, PDE4D4 and PDE4D5 are readily detected in 4D3NT-V5 IP pellets, whereas short variants PDE4D1 and PDE4D2 do not interact with 4D3NT-V5. This finding suggests that long PDE4D variants may also form hetero-oligomers. Co-IP of long PDE4s is not only detected among the variants generated from the same gene, but also between variants expressed from different PDE4 genes. As shown in Figure 3B, long PDE4A variants co-

immunoprecipitate with long PDE4D variants, whereas short PDE4A and short PDE4D variants neither interact with one another nor with the long forms. In line with the idea that co-immunoprecipitation of long PDE4s is due to hetero-dimerization, ablation of dimerization by nested deletion of UCR1C also ablates co-IP of PDE4 long forms (Supplementary Figure S2.). Together, these data suggest that in addition to homo-oligomers, long PDE4 variants form hetero-oligomers *via* their N-terminal UCR domains.

PDE4 oligomerization is not subject to rapid dissociation/reassociation

To assess the dynamics of PDE4 oligomerization, we compared the efficiency of the pull-down of differentially tagged PDE4D3 constructs that had been either co-expressed in the same cells or had been expressed on separate cell culture plates followed by combination of the cell extracts after cell harvest and rotation of the mixture at 4°C for 24 h. As shown in Figure 4, oligomerization of PDE4 is detected by co-IP only when the variants are co-expressed in the same cells, but not when they were expressed in different cells. This indicates that PDE4 hetero-oligomers are formed within cells prior to cell lysis and that once formed, oligomers are not subject to significant levels of dissociation/reassociation *in vitro*. This finding is also consistent with the lack of monomeric species of PDE4 long forms in size-exclusion chromatography and/or density gradients (Figure 1D/E).

Detection of PDE4 hetero-oligomers in living cells

To investigate PDE4 hetero-oligomerization in intact cells, we next utilized a Förster resonance energy transfer (FRET)-based approach. To this end, the UCR regions of PDE4D and/or PDE4A were fused C-terminally with the FRET-donor GFP or the FRET-acceptor RFP (Figure 5A). FRET is detected when GFP- and RFP-tagged constructs are sequestered in close proximity, thereby allowing energy transfer from GFP to RFP. As shown in Figure 5B/C, co-expression of GFP or the N-terminal region of PDE4D fused to GFP (4DNT-GFP) with RFP does not produce FRET. Conversely, co-expression of constructs encoding for PDE4D and/or PDE4A fusion proteins differentially tagged with GFP and/or RFP does induce FRET in line with the idea that these probes form homo- and/or hetero-oligomers *in vivo*. The signal intensity for both fluorophores as well as the FRET signal is widely dispersed throughout the cells suggesting that detection of oligomerization by FRET is not due to enrichment of the probes in specific subcellular compartments. These data indicate that the UCR domains are sufficient to mediate both homo- and/or hetero-oligomerization in an intact cell.

Detection of hetero-oligomers formed by endogenous PDE4

Next, we wished to explore whether exogenous PDE4s form hetero-oligomers with endogenous enzymes. To this end, constructs 4D3NT-V5, encoding the UCR regions of PDE4D3, and 4D3dead-V5, encoding a catalytically inactive full-length PDE4D3, were expressed in Hek293 cells and subsequently immunoprecipitated *via* their C-terminal V5-tags. The IP pellets were then probed for the presence of endogenous PDE4. As shown in Figure 6, significant amounts of PDE activity are recovered in IP pellets from cells expressing 4D3NT-V5 or 4D3dead-V5, compared to mock-transfected controls, and this activity is ablated in the presence of the PDE4-selective inhibitor rolipram. This suggests

that exogenous PDE4 can form hetero-oligomers with endogenous PDE4, but not with PDEs other than PDE4. Next, we probed whether endogenous PDE4s form hetero-oligomers among themselves by co-immunoprecipitation of PDE4s from lysates of mouse brains; using brains from PDE4B$^{-/-}$ and PDE4D$^{-/-}$ mice, which have been described previously [20, 21], as controls (Figure 7). As shown in Figure 7A, multiple isoforms of PDE4A, PDE4B and PDE4D are expressed in mouse brain. We then immunoprecipitated PDE4D with subtype-selective antibodies and probed for the presence of PDE4A and PDE4B in IP pellets by Western blotting. As shown in Figure 7B, both long PDE4A and PDE4B variants can be detected in PDE4D-IP pellets, but not in IPs with normal IgG used as control. Co-IP of PDE4A or PDE4B is not detected in IPs from PDE4D$^{-/-}$ brains excluding the possibility of an unspecific pull down due to cross-reactivity with the PDE4D antibody. As shown in Figure 7A, two immunoreactive bands for PDE4A are detected in brain, one representing the short form PDE4A1 and the other various PDE4A long variants. As shown in Figure 7B/C, only the long, but not the short PDE4A variant(s) are detected in PDE4D IP pellets in line with the idea that co-IP is due to UCR1/2-dependent hetero-oligomerization. That PDE4 oligomers do not dissociate/re-associate *in vitro*, as suggested from the data in Figures 1 and 4, provides the opportunity to quantify the fraction of endogenous PDE4 present as hetero-oligomers. To this end, the amount of PDE4A detected in PDE4D IP pellets was quantified and compared to the total amount of PDE4A in the lysates used as input for the IP. As shown in Figure 7C, ~2% of the endogenous PDE4A expressed in brain was found in complex with PDE4D suggesting that hetero-oligomers constitute a minor fraction of the total PDE4 proteins expressed in mouse brain. Given that the expression patterns of individual PDE4 subtypes in the brain are distinct at the regional and cellular level, individual cells might contain somewhat higher or lower levels of PDE4 hetero-oligomers simply as a result of different amounts of the interacting PDE4 subtypes being expressed.

PDE4 hetero-oligomerization mediates novel protein interaction networks

Numerous PDE4 protein/protein interactions have now been reported. Interestingly, none of the established PDE4 interaction sites include the UCR1C/UCR2N regions that mediate dimerization. This could suggest that dimerization is not a prerequisite for these protein/protein interactions, and that the two long form protomers may mediate independent protein interactions. To test this idea, we probed whether hetero-oligomerization could sequester PDE4D to a signaling complex unique to PDE4A; the interaction of PDE4A with the SH3 domain of Lyn kinase (Lyn/SH3) [22, 23]. As shown in Figure 8, PDE4A4 binds to Lyn/SH3, an interaction mediated by its variant-specific amino terminus and the linker region between UCR2 and the catalytic domain. Ablation of dimerization *via* nested deletion of UCR1C does not ablate the interaction of 4A4ΔUCR1C with Lyn/SH3 (Figure 8/Lane 8), suggesting that it is independent of the state of oligomerization. PDE4D does not bind to Lyn/SH3 by itself. However, if co-expressed with PDE4A in Hek293 cells, PDE4D is recovered in Lyn/SH3 IP pellets. Conversely, co-expression with the monomeric 4A4ΔUCR1C construct does not sequester PDE4D to the Lyn/SH3 complex. Together, these data indicate that hetero-oligomerization allows for the generation of novel protein complexes.

DISCUSSION

Over recent years, our understanding of the functions of PDE4s in the body has advanced rapidly. PDE4s have been identified as critical regulators of cAMP signaling in distinct subcellular compartments of many cells and tissues, and individual PDE4 subtypes and variants have been associated with a plethora of unique physiological and pathophysiological phenotypes [1, 2, 10]. Still, the structural organization of PDE4s that allows for these critical and diverse functions remains less well-defined. This is particularly true for the UCR domains. To date, no atomic structures of a full-length PDE4 or the isolated UCR1/UCR2 module are available and the mechanisms by which the UCRs control enzyme activity and inhibitor sensitivity of PDE4s remain unclear.

Here, we have determined one important facet of UCR function. We demonstrate that the properties of long and short PDE4 variants are defined by distinct quaternary structures. Determination of molecular weights of distinct PDE4 long and short forms by size exclusion chromatography and density gradient centrifugation as well as co-IP experiments suggest that as a general rule, PDE4 short forms behave as monomers, whereas PDE4 long forms exist as dimers (Figures 1–3). The UCR domains were found to mediate the critical intermolecular interactions that allow for dimerization of long forms. This conclusion is supported by the observation that deletions within the UCR domains ablate dimerization (Figure 2), and that the isolated UCR domains can oligomerize by themselves (Figures 3A, 5 and 6). Furthermore, through FRET microscopy (Figure 5) and co-IP of exogenous and/or endogenous PDE4 (Figures 3, 6 and 7), we demonstrate that the UCR domains are not only capable of mediating homo-oligomerization, but also hetero-oligomerization of distinct PDE4 long forms.

In addition to PDE4 long forms, multiple other PDEs, including PDE2, PDE3, PDE5, PDE6 and PDE11 have been shown to form dimers [11, 12, 24–31]. Although the primary structure of the N-terminal regions of different PDEs are highly divergent, their role in mediating dimerization appears conserved. N-terminal truncation has been shown to ablate dimerization of PDE4, PDE5 and PDE11 [11, 24, 27] and electron-microscopic images of PDE5 and PDE6 [32, 33] as well as the crystal structure of PDE2 [25] further confirm a critical role of their respective N-termini in enzyme dimerization.

With the exception of the retinal rod PDE6 [30], dimerization is not required for catalytic activity of PDEs and N-terminally truncated, monomeric PDE constructs or even the isolated catalytic domains *per se* retain full enzyme activity. Dimerization is critical, however, for the regulation of enzyme activity. In particular, many PDEs are activated by phosphorylation, or allosteric binding of ligands at the N-terminal domains [1]. These include binding of cAMP and/or cGMP to the GAF domains in PDE2, PDE5, PDE6 and PDE10 [29, 34–36] and phosphatidic acid binding to the UCR1 of PDE4 [6, 7] as well as the activation of PDEs by phosphorylation including the PKA and PKG-mediated activation of PDE4 and PDE5 [3, 37, 38]. The crystal structure of PDE2 reported by Pandit and colleagues provides both a model for the regulation of enzyme activity by modulation of the N-terminal domains as well as an explanation for the requirement of PDE dimerization [25]. In PDE2, interactions between the N-terminal GAF domains are critical for stacking the

substrate binding sites at the catalytic domain against each other, thus preventing substrate access. cGMP-binding to the N-terminal GAF domains induces conformational changes that release this block by slightly moving the active sites away from each other. This model agrees with multiple other observations of PDE regulation, such as the release of an inhibitory constraint on the active site *via* proteolytic digest of the UCR domains in PDE4 [39], and likely represents a general model for PDE activation. Conversely, how the activity of the monomeric short PDE4 forms is regulated by post-translational modifications, such as ERK2 phosphorylation [8, 9], remains to be established. Although (homo-)dimerization is thus well established as critical for the regulation of enzyme activity, the functional significance of hetero-oligomerization of PDEs is less clear. The exception is the retinal rod PDE6 [30], which is an anomaly among the PDEs, in that it is functional only as a hetero-dimer between two subunits, PDE6A and PDE6B, expressed from distinct genes. Conversely, the cone PDE6, PDE6C, forms homodimers [30].

The finding that distinct PDE4 subtypes and variants associate in hetero-oligomers appears in conflict with some established properties of these enzymes. Many protein/protein interactions involving PDE4s are unique to individual PDE4 subtypes and/or variants [10]. In addition, we and others have shown that PDE4s can be selectively immunoprecipitated with subtype- or variant-selective antibodies [13, 18]. Both findings conflict with the idea that distinct PDE4s are physically associated with one another. Our finding that the amount of PDE4 hetero-oligomers is minor, compared to that of homo-dimers, resolves this conflict. Why only a low fraction of PDE4s form hetero-oligomers remains to be determined. The fact that we do not detect monomeric species of PDE4 long forms in size exclusion chromatography and density gradients (Figure 1) and that PDE4s do not dissociate/reassociate *in vitro* (Figure 4) may suggest that the PDE dimer interaction has a very high affinity. If so, dimers may form quickly and irreversibly upon protein synthesis. In this context, homo-dimerization might be preferred simply by the fact that an amino acid chain translated from the same mRNA is the most readily available interaction partner. However, other mechanisms that could favor homo-oligomerization, such as a role of chaperones or an impact of the non-conserved sequences flanking the UCR domains, might also exist.

Recent studies suggest that PDE4s may act as scaffolding proteins [10, 40, 41], thus exerting functions independent of their catalytic activity, by mediating the assembly of macromolecular signaling complexes. The ability of PDE4 protomers to engage in independent protein interactions may support scaffolding function of PDEs and hetero-oligomerization may allow for further complexity in protein interactions (see Figure 8). The physiological significance of protein complexes formed by endogenous PDE4 hetero-oligomers remains to be established. The more immediate application of our findings concerns the overexpression of catalytically inactive PDE4 constructs to displace endogenous PDE4 from signaling complexes. Our findings (see Figure 6) suggest that expression of these dominant-negative constructs may act in part by scavenging newly synthesized endogenous PDE4 long forms *via* hetero-oligomerization, in addition to displacing them from signaling complexes.

With the exception of the rod PDE6, which is functional only as a hetero-dimer, hetero-oligomerization of PDEs has not been reported before. However, given our current findings

on PDE4 and the fact that most PDEs are expressed as multiple variants and dimerize *via* conserved N-terminal domains, it is likely that PDE hetero-oligomerization might be more common than thus far appreciated.

Supplementary Material

Refer to Web version on PubMed Central for supplementary material.

Acknowledgments

FUNDING

This work was supported by National Institutes of Health grants HL092788, HL107960 and DK072517. E.B. is supported by an Elizabeth Nash Postdoc fellowship from Cystic Fibrosis Research Incorporated (CFRI).

Abbreviations

ERK	extracellular signal-regulated kinase
FRET	Förster resonance energy transfer
GAF	cGMP-activated PDEs, adenylyl cyclase, and Fh1A
GFP	green fluorescent protein
GST	glutathione S-transferase
IP	immunoprecipitation
PDE(s)	cyclic nucleotide phosphodiesterase(s)
PKA	protein kinase A
PKG	protein kinase G
RFP	red fluorescent protein
SH3 domain	Src homology 3 domain
UCR	upstream conserved region

References

1. Conti M, Beavo J. Biochemistry and physiology of cyclic nucleotide phosphodiesterases: essential components in cyclic nucleotide signaling. Annu Rev Biochem. 2007; 76:481–511. [PubMed: 17376027]
2. Conti M, Richter W, Mehats C, Livera G, Park JY, Jin C. Cyclic AMP-specific PDE4 phosphodiesterases as critical components of cyclic AMP signaling. J Biol Chem. 2003; 278:5493–5496. [PubMed: 12493749]
3. Sette C, Conti M. Phosphorylation and activation of a cAMP-specific phosphodiesterase by the cAMP-dependent protein kinase. Involvement of serine 54 in the enzyme activation. J Biol Chem. 1996; 271:16526–16534. [PubMed: 8663227]
4. MacKenzie SJ, Baillie GS, McPhee I, MacKenzie C, Seamons R, McSorley T, Millen J, Beard MB, van Heeke G, Houslay MD. Long PDE4 cAMP specific phosphodiesterases are activated by protein kinase A-mediated phosphorylation of a single serine residue in Upstream Conserved Region 1 (UCR1). Br J Pharmacol. 2002; 136:421–433. [PubMed: 12023945]

5. Bruss MD, Richter W, Horner K, Jin SL, Conti M. Critical role of PDE4D in beta2-adrenoceptor-dependent cAMP signaling in mouse embryonic fibroblasts. J Biol Chem. 2008; 283:22430–22442. [PubMed: 18508768]

6. Grange M, Sette C, Prigent AF, Lagarde M, Némoz G. Regulation of cAMP-phosphodiesterases by phosphatidic acid binding. Lipids. 1999; 34(Suppl):S83. [PubMed: 10419099]

7. Grange M, Sette C, Cuomo M, Conti M, Lagarde M, Prigent AF, Némoz G. The cAMP-specific phosphodiesterase PDE4D3 is regulated by phosphatidic acid binding. Consequences for cAMP signaling pathway and characterization of a phosphatidic acid binding site. J Biol Chem. 2000; 275:33379–33387. [PubMed: 10938092]

8. Baillie GS, MacKenzie SJ, McPhee I, Houslay MD. Sub-family selective actions in the ability of Erk2 MAP kinase to phosphorylate and regulate the activity of PDE4 cyclic AMP-specific phosphodiesterases. Br J Pharmacol. 2000; 131:811–819. [PubMed: 11030732]

9. Hoffmann R, Baillie GS, MacKenzie SJ, Yarwood SJ, Houslay MD. The MAP kinase ERK2 inhibits the cyclic AMP-specific phosphodiesterase HSPDE4D3 by phosphorylating it at Ser579. EMBO J. 1999; 18:893–903. [PubMed: 10022832]

10. Houslay MD. Underpinning compartmentalised cAMP signalling through targeted cAMP breakdown. Trends Biochem Sci. 2010; 35:91–100. [PubMed: 19864144]

11. Richter W, Conti M. Dimerization of the type 4 cAMP-specific phosphodiesterases is mediated by the upstream conserved regions (UCRs). J Biol Chem. 2002; 277:40212–40221. [PubMed: 12177055]

12. Richter W, Conti M. The oligomerization state determines regulatory properties and inhibitor sensitivity of type 4 cAMP-specific phosphodiesterases. J Biol Chem. 2004; 279:30338–30348. [PubMed: 15131123]

13. Richter W, Jin SL, Conti M. Splice variants of the cyclic nucleotide phosphodiesterase PDE4D are differentially expressed and regulated in rat tissue. Biochem J. 2005; 388:803–811. [PubMed: 15717866]

14. Richter W, Xie M, Scheitrum C, Krall J, Movsesian MA, Conti M. Conserved expression and functions of PDE4 in rodent and human heart. Basic Res Cardiol. 2011; 106:249–262. [PubMed: 21161247]

15. Campbell RE, Tour O, Palmer AE, Steinbach PA, Baird GS, Zacharias DA, Tsien RY. A monomeric red fluorescent protein. Proc Natl Acad Sci U S A. 2002; 99:7877–7882. [PubMed: 12060735]

16. Richter W. Determining the subunit structure of phosphodiesterases using gel filtration and sucrose density gradient centrifugation. Methods Mol Biol. 2005; 307:167–180. [PubMed: 15988063]

17. Siegel LM, Monty KJ. Determination of molecular weights and frictional ratios of proteins in impure systems by use of gel filtration and density gradient centrifugation. Application to crude preparations of sulfite and hydroxylamine reductases. Biochim Biophys Acta. 1966; 112:346–362. [PubMed: 5329026]

18. Richter W, Day P, Agrawal R, Bruss MD, Granier S, Wang YL, Rasmussen SG, Horner K, Wang P, Lei T, Patterson AJ, Kobilka B, Conti M. Signaling from beta1- and beta2-adrenergic receptors is defined by differential interactions with PDE4. EMBO J. 2008; 27:384–393. [PubMed: 18188154]

19. Huston E, Gall I, Houslay TM, Houslay MD. Helix-1 of the cAMP-specific phosphodiesterase PDE4A1 regulates its phospholipase-D-dependent redistribution in response to release of Ca2+ J Cell Sci. 2006; 119:3799–3810. [PubMed: 16940352]

20. Jin SL, Richard FJ, Kuo WP, D'Ercole AJ, Conti M. Impaired growth and fertility of cAMP-specific phosphodiesterase PDE4D-deficient mice. Proc Natl Acad Sci U S A. 1999; 96:11998–12003. [PubMed: 10518565]

21. Jin SL, Conti M. Induction of the cyclic nucleotide phosphodiesterase PDE4B is essential for LPS-activated TNF-alpha responses. Proc Natl Acad Sci U S A. 2002; 99:7628–7633. [PubMed: 12032334]

22. Beard MB, Huston E, Campbell L, Gall I, McPhee I, Yarwood S, Scotland G, Houslay MD. In addition to the SH3 binding region, multiple regions within the N-terminal noncatalytic portion of

the cAMP-specific phosphodiesterase, PDE4A5, contribute to its intracellular targeting. Cell Signal. 2002; 14:453–465. [PubMed: 11882390]

23. McPhee I, Yarwood SJ, Scotland G, Huston E, Beard MB, Ross AH, Houslay ES, Houslay MD. Association with the SRC family tyrosyl kinase LYN triggers a conformational change in the catalytic region of human cAMP-specific phosphodiesterase HSPDE4A4B. Consequences for rolipram inhibition. J Biol Chem. 1999; 274:11796–11810. [PubMed: 10206997]
24. Fink TL, Francis SH, Beasley A, Grimes KA, Corbin JD. Expression of an active, monomeric catalytic domain of the cGMP-binding cGMP-specific phosphodiesterase (PDE5). J Biol Chem. 1999; 274:34613–34620. [PubMed: 10574925]
25. Pandit J, Forman MD, Fennell KF, Dillman KS, Menniti FS. Mechanism for the allosteric regulation of phosphodiesterase 2A deduced from the X-ray structure of a near full-length construct. Proc Natl Acad Sci U S A. 2009; 106:18225–18230. [PubMed: 19828435]
26. Kenan Y, Murata T, Shakur Y, Degerman E, Manganiello VC. Functions of the N-terminal region of cyclic nucleotide phosphodiesterase 3 (PDE 3) isoforms. J Biol Chem. 2000; 275:12331–12338. [PubMed: 10766874]
27. Weeks JL, Zoraghi R, Francis SH, Corbin JD. N-Terminal domain of phosphodiesterase-11A4 (PDE11A4) decreases affinity of the catalytic site for substrates and tadalafil, and is involved in oligomerization. Biochemistry. 2007; 46:10353–10364. [PubMed: 17696499]
28. Martins TJ, Mumby MC, Beavo JA. Purification and characterization of a cyclic GMP-stimulated cyclic nucleotide phosphodiesterase from bovine tissues. J Biol Chem. 1982; 257:1973–1979. [PubMed: 6276403]
29. Martinez SE, Wu AY, Glavas NA, Tang XB, Turley S, Hol WG, Beavo JA. The two GAF domains in phosphodiesterase 2A have distinct roles in dimerization and in cGMP binding. Proc Natl Acad Sci U S A. 2002; 99:13260–13265. [PubMed: 12271124]
30. Muradov KG, Boyd KK, Martinez SE, Beavo JA, Artemyev NO. The GAFa domains of rod cGMP-phosphodiesterase 6 determine the selectivity of the enzyme dimerization. J Biol Chem. 2003; 278:10594–10601. [PubMed: 12531898]
31. Zoraghi R, Bessay EP, Corbin JD, Francis SH. Structural and functional features in human PDE5A1 regulatory domain that provide for allosteric cGMP binding, dimerization, and regulation. J Biol Chem. 2005; 280:12051–12063. [PubMed: 15677448]
32. Kameni Tcheudji JF, Lebeau L, Virmaux N, Maftei CG, Cote RH, Lugnier C, Schultz P. Molecular organization of bovine rod cGMP-phosphodiesterase 6. J Mol Biol. 2001; 310:781–791. [PubMed: 11453687]
33. Kajimura N, Yamazaki M, Morikawa K, Yamazaki A, Mayanagi K. Three-dimensional structure of non-activated cGMP phosphodiesterase 6 and comparison of its image with those of activated forms. J Struct Biol. 2002; 139:27–38. [PubMed: 12372317]
34. Rybalkin SD, Rybalkina IG, Shimizu-Albergine M, Tang XB, Beavo JA. PDE5 is converted to an activated state upon cGMP binding to the GAF A domain. EMBO J. 2003; 22:469–478. [PubMed: 12554648]
35. Jäger R, Russwurm C, Schwede F, Genieser HG, Koesling D, Russwurm M. Activation of PDE10 and PDE11 phosphodiesterases. J Biol Chem. 2012; 287:1210–1219. [PubMed: 22105073]
36. Gross-Langenhoff M, Hofbauer K, Weber J, Schultz A, Schultz JE. cAMP is a ligand for the tandem GAF domain of human phosphodiesterase 10 and cGMP for the tandem GAF domain of phosphodiesterase 11. J Biol Chem. 2006; 281:2841–2846. [PubMed: 16330539]
37. Corbin JD, Francis SH. Cyclic GMP phosphodiesterase-5: target of sildenafil. J Biol Chem. 1999; 274:13729–13732. [PubMed: 10318772]
38. Bessay EP, Blount MA, Zoraghi R, Beasley A, Grimes KA, Francis SH, Corbin JD. Phosphorylation increases affinity of the phosphodiesterase-5 catalytic site for tadalafil. J Pharmacol Exp Ther. 2008; 325:62–68. [PubMed: 18199808]
39. Lim J, Pahlke G, Conti M. Activation of the cAMP-specific phosphodiesterase PDE4D3 by phosphorylation. Identification and function of an inhibitory domain. J Biol Chem. 1999; 274:19677–19685. [PubMed: 10391907]
40. Day JP, Lindsay B, Riddell T, Jiang Z, Allcock RW, Abraham A, Sookup S, Christian F, Bogum J, Martin EK, Rae RL, Anthony D, Rosair GM, Houslay DM, Huston E, Baillie GS, Klussmann E,

Houslay MD, Adams DR. Elucidation of a structural basis for the inhibitor-driven, p62 (SQSTM1)-dependent intracellular redistribution of cAMP phosphodiesterase-4A4 (PDE4A4). J Med Chem. 2011; 54:3331–3347. [PubMed: 21456625]

41. Murdoch H, Vadrevu S, Prinz A, Dunlop AJ, Klussmann E, Bolger GB, Norman JC, Houslay MD. Interaction between LIS1 and PDE4, and its role in cytoplasmic dynein function. J Cell Sci. 2011; 124:2253–2266. [PubMed: 21652625]

Summary Statement

PDE4s are divided into long and short variants by the presence or absence of the N-terminal UCR domains. The UCRs mediate homo- as well as hetero-oligomerization of long PDE4s, whereas short variants, which lack portions of the UCRs, are monomers.

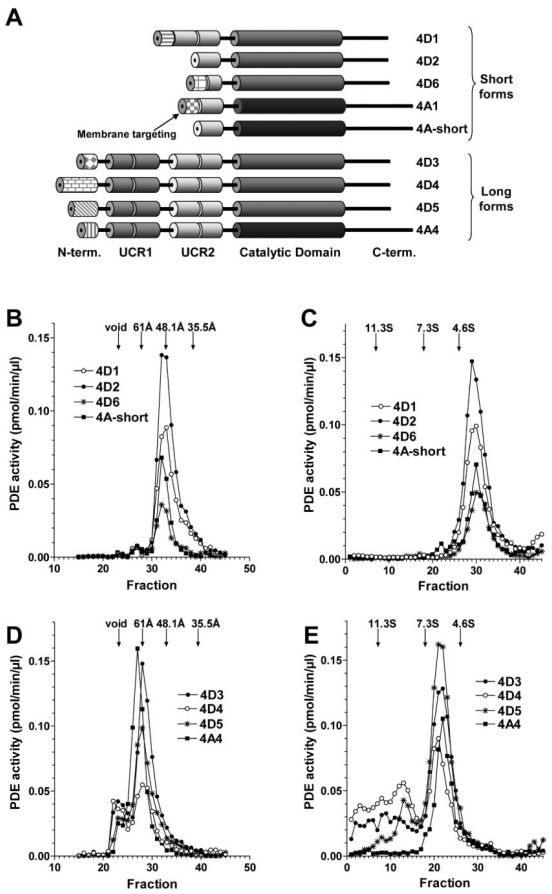

Figure 1. PDE4 long forms are dimers, whereas short forms are monomers

(**A**) domain organization of the PDE4 variants analyzed in (**B–E**). Domains are depicted as *barrels* connected by *wires* (putative linker regions). Long forms contain the complete UCR1/UCR2 module, whereas short forms lack UCR1 but still contain a part of, or the entire UCR2. (**B–E**) determination of apparent molecular weights of short (4D1, 4D2, 4D6 and 4A-short; **B/C**) and long (4D3, 4D4, 4D5 and 4A4; **D/E**) PDE4 variants exogenously expressed in COS7 cells by size exclusion chromatography (**B/D**) and sucrose density gradient centrifugation (**C/E**), respectively. The Stokes radii and/or sedimentation coefficients of several molecular weight standard proteins separated under identical conditions are indicated with arrows. All data are representative of experiments performed three times.

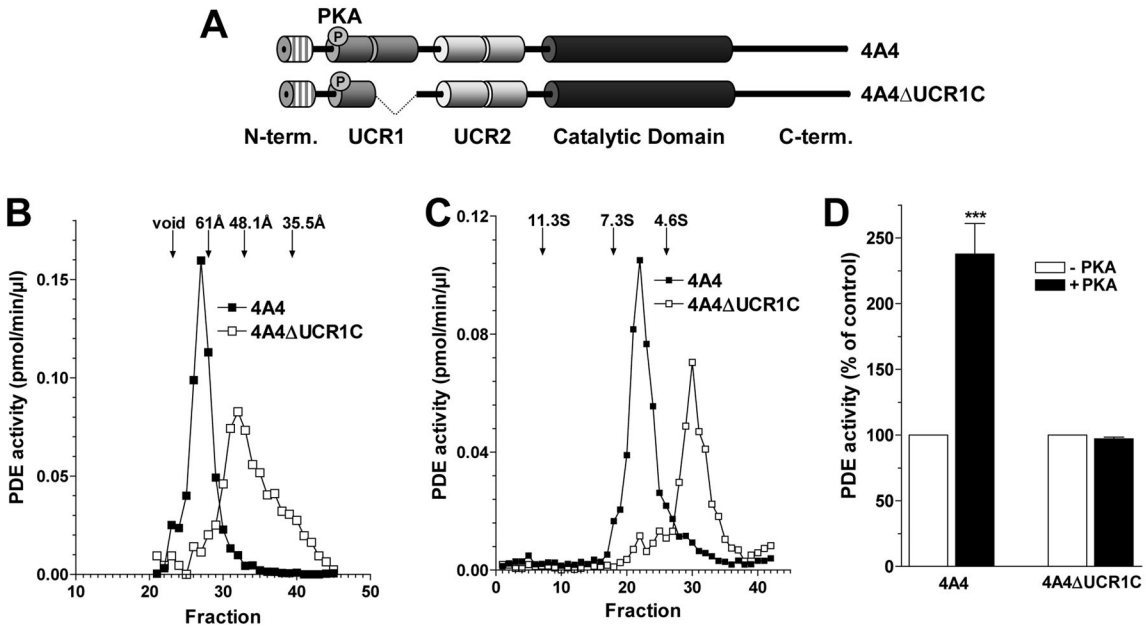

Figure 2. The C-terminal half of UCR1 is required for dimerization of PDE4A4

(**A**) scheme illustrating the domain organization of PDE4A4 and a 4A4 construct lacking the C-terminal half of UCR1 (4A4ΔUCR1C). (**B**/**C**) PDE4A4 and 4A4ΔUCR1C, exogenously expressed in COS7 cells, were subjected to size exclusion chromatography (**B**) and density gradient centrifugation (**C**). Nested deletion of UCR1C causes a shift in elution/migration reflecting a loss of dimerization (Stokes radii are 65 and 51 Å and Sedimentation coefficients are 6.4 and 3.7 S for 4A4 and 4A4ΔUCR1C, respectively). (**D**) exogenous 4A4 and 4A4ΔUCR1C were subjected to *in vitro* PKA phosphorylation assays. Deletion of UCR1C ablates the PKA-mediated activation of 4A4. Data are representative of (**B**/**C**) or represent the mean ± s.e.m. (**D**) of experiments performed three times. ***, $p<0.001$

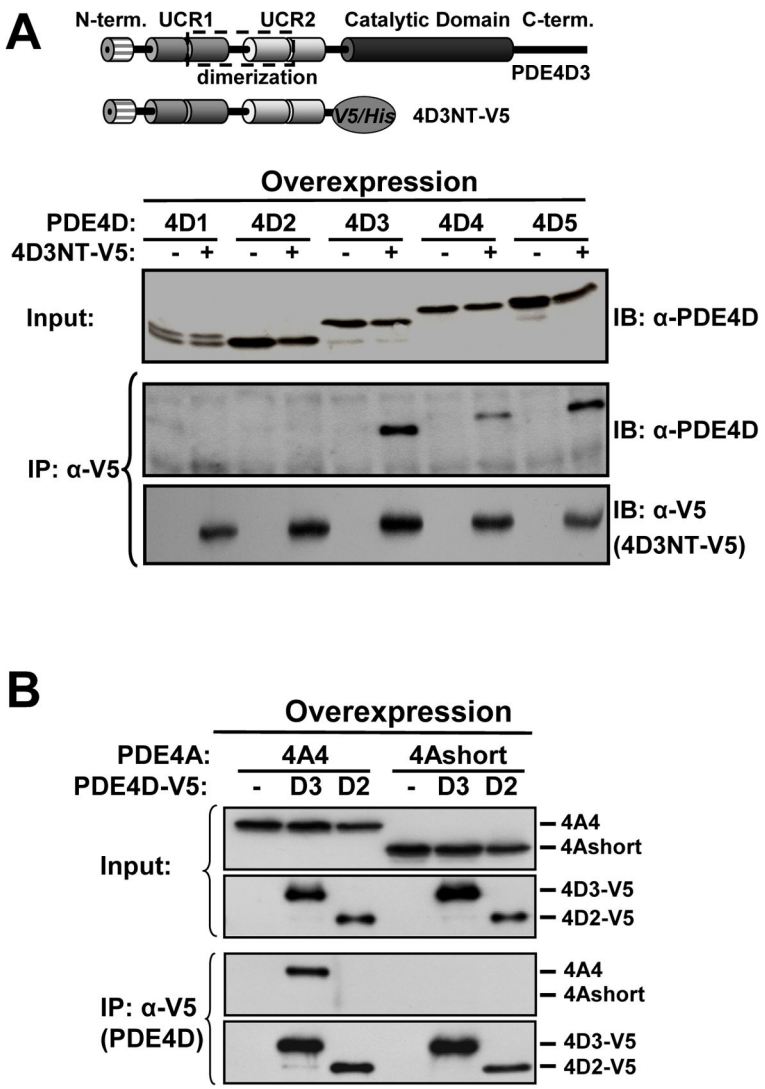

Figure 3. Hetero-oligomerization of long PDE4 variants detected by co-IP of exogenous proteins

(**A**) short variants 4D1 and 4D2 as well as long variants 4D3, 4D4 and Myc-tagged 4D5 were expressed in COS7 cells either by themselves or co-expressed with the construct 4D3NT-V5 encoding the N-terminal domain of PDE4D3 fused to a V5-tag (see scheme on top). After cell harvest, 4D3NT-V5 was immunoprecipitated from the cell homogenates and the IP pellet was probed for the presence of the full-length PDE4 variants by Western blotting. (**B**) PDE4A constructs 4A4 and 4Ashort were expressed in COS7 cells either by themselves or co-expressed with V5-tagged PDE4D constructs 4D2-V5 or 4D3-V5. After cell harvest, the PDE4D variants were immunoprecipitated using V5-antibody and the IP pellets probed for the presence of PDE4A variants. Only co-expression of the two long variants 4A4 and 4D3 generates hetero-oligomers, whereas short forms 4Ashort and/or 4D2 do not interact with one another or with the long PDE4 variants, respectively. Western blots are representative of experiments performed three times.

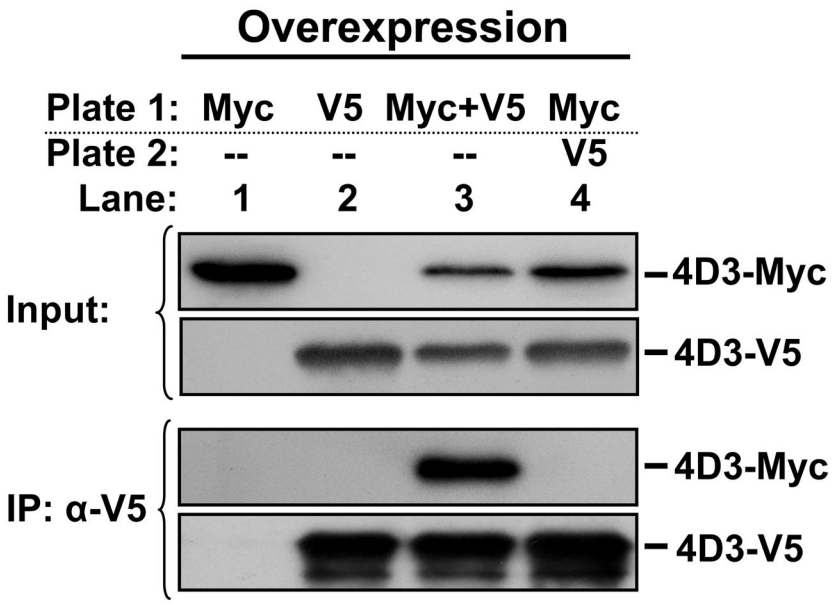

Figure 4. PDE4 oligomers do not dissociate/reassociate *in vitro*

PDE4D3 constructs, differentially tagged with either V5- or Myc-tags, were transfected in COS7 cells either separately (lanes 1, 2 and 4) or co-transfected together onto the same cell culture plate (lane 3). After cell harvest, lysates from two cell culture plates were combined as indicated, the mixture rotated for 24 h at 4°C and then subjected to IP with α-V5 antibody. PDE4D proteins in the cell lysates used as IP input (two upper panels) or recovered in IP pellets (two lower panels) were detected by Western blotting.

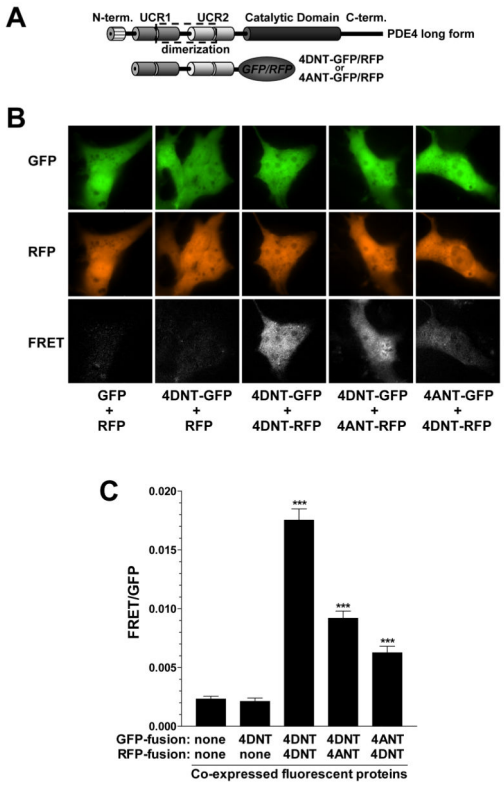

Figure 5. The UCR domains mediate oligomerization in intact cells

Vectors encoding GFP, RFP or chimeras of these two fluorescent proteins with the UCR domains of PDE4A or PDE4D were co-expressed in COS7 cells. (**A**) scheme illustrating the domain organization of the PDE4-GFP/RFP chimeras used, compared to that of full-length PDE4. (**B**) representative images showing GFP, RFP and FRET intensities of transfected COS7 cells. (**C**) quantification of FRET intensity of different PDE4-GFP/RFP chimeras. Data represent mean ± s.e.m. of n ≥37 cells. ***, $p<0.001$

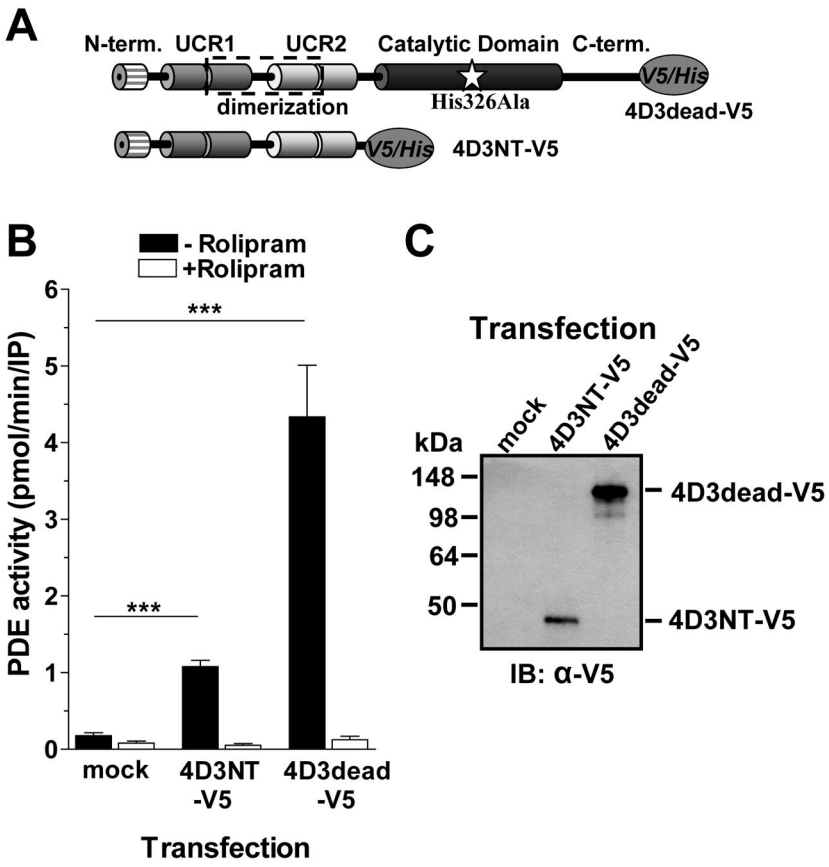

Figure 6. Hetero-oligomers formed between exogenous and endogenous PDE4

Cell extracts prepared from Hek293 cells transfected with PDE4 constructs 4D3NT-V5, 4D3dead-V5 or empty vector (mock) were subjected to IP with α-V5 antibodies. (**A**) scheme illustrating the domain organization of 4D3NT-V5 and 4D3dead-V5, a full length, catalytically inactive PDE4D3 carrying a point mutation (His326Ala) in the catalytic domain. (**B**) shown is the PDE activity recovered in α-V5 IP pellets measured in the presence or absence of the PDE4-selective inhibitor rolipram (10 μM). Data represent the mean ± s.e.m. of three experiments. (**C**) immuno blot showing 4D3NT-V5 and 4D3dead-V5 recovered in α-V5 IP pellets. The level of 4D3NT-V5 expression was consistently lower than that of 4D3dead-V5 in all experiments.

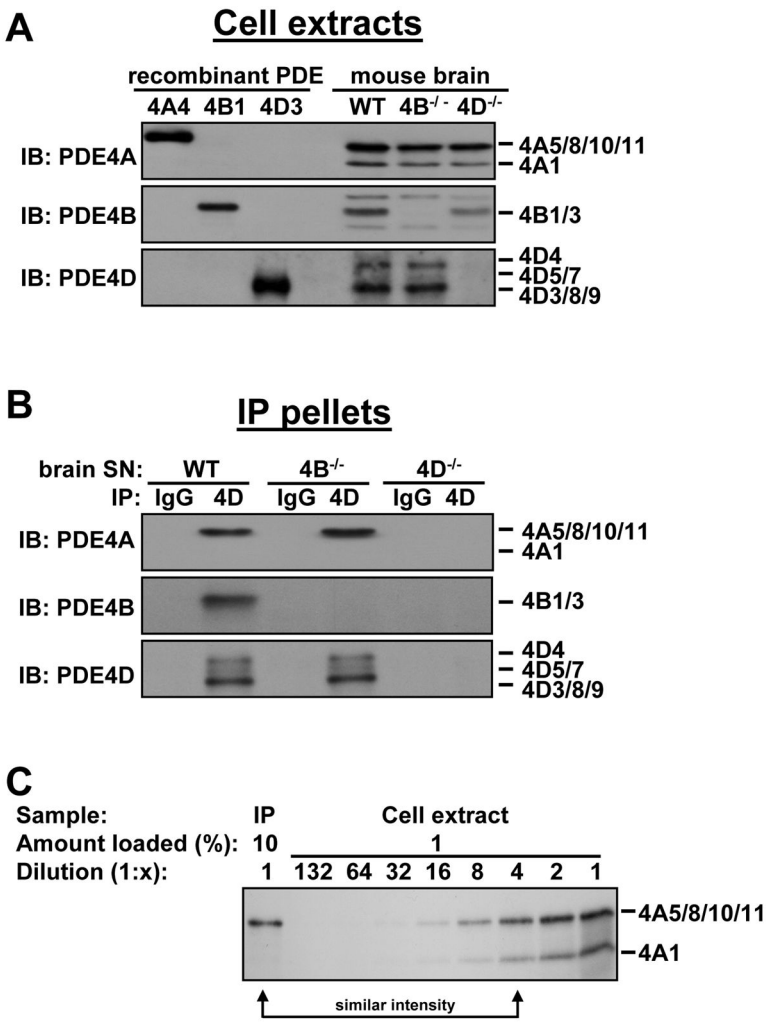

Figure 7. Hetero-oligomers formed by endogenous PDE4s

Detergent extracts prepared from whole brains of wild type (WT), PDE4B$^{-/-}$ and PDE4D$^{-/-}$ mice were subjected to IP with α-PDE4D antibodies or normal IgG as a control. (**A**) detection of PDE4A, PDE4B and PDE4D variants in the tissue extracts used as IP inputs compared to recombinant PDE4 variants. We detect two immunoreactive bands (110 and 75 kDa) for PDE4A. Based on their migration, they likely represent long variants PDE4A5/8/10/11 and the short variant PDE4A1, respectively. We detect one immunoreactive band for PDE4B (95 kDa), likely representing PDE4B1 and/or PDE4B3, and three immunoreactive bands for PDE4D (106, 99 and 90 kDa), representing multiple PDE4D long forms as indicated. (**B**) shown are the PDE4 variants recovered in the α-PDE4D IP pellets. (**C**) quantification of the amount of PDE4A detected in PDE4D IP pellets. The left lane shows 10% of the total protein recovered in an α-PDE4D IP pellet. Its immunoblot intensity is compared to 1% (as well as several further dilutions) of the amount of supernatant used as IP input. In the example shown, the intensity of the 10% IP band corresponds to ~ 0.25% of the supernatant, indicating that ~2.5% of the total PDE4 long form in the IP input co-immunoprecipitated with PDE4D.

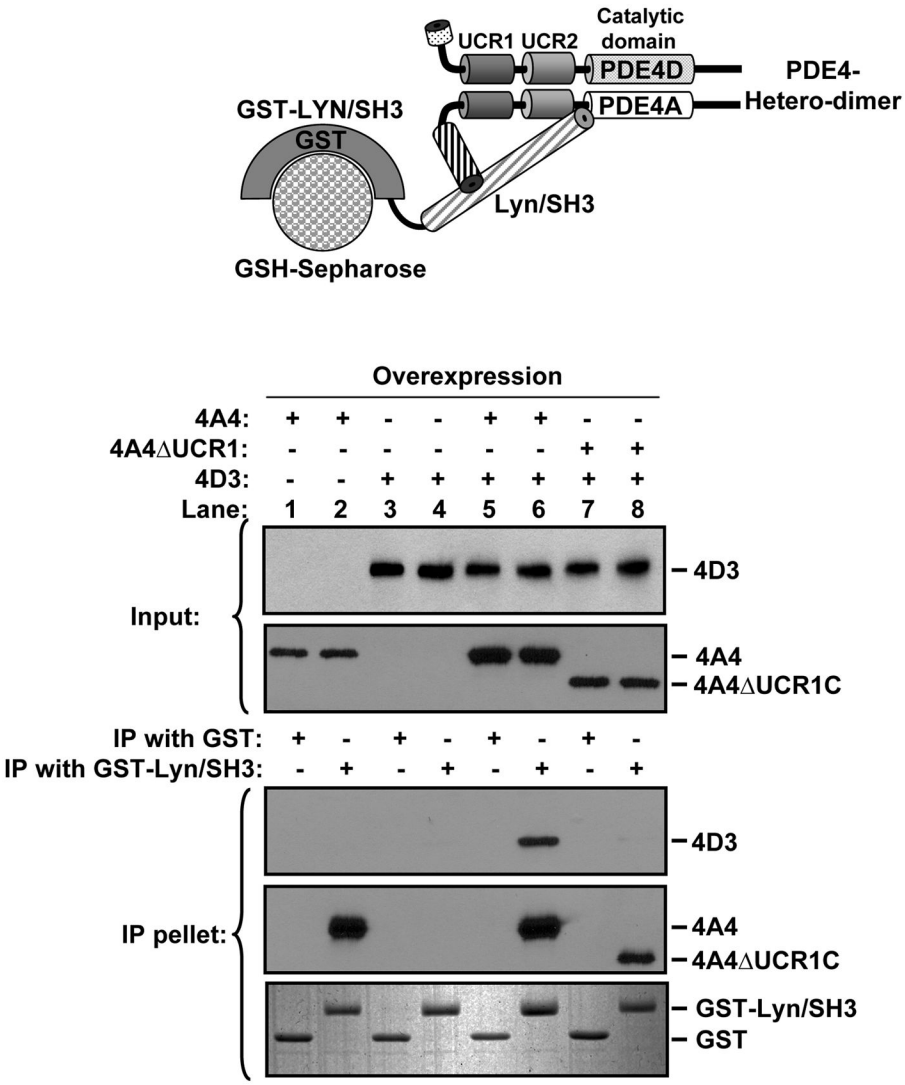

Figure 8. Hetero-oligomerization generates novel PDE4 protein interaction networks

Long PDE4 variants 4D3 and 4A4 as well as 4A4ΔUCR1C, a monomeric 4A4 resulting from nested deletion of UCR1C, were expressed in Hek293 cells either separately (lanes 1–4) or co-expressed on the same plate (lanes 5–8). After cell harvest, cell extracts were mixed with equal amounts of GST (lanes 1, 3, 5, 7) or GST-Lyn/SH3 (lanes 2, 4, 6 and 8), a GST fusion protein encoding the SH3 domain of Lyn kinase, which selectively binds to 4A4 *via* its N-terminus and UCR2/catalytic domain linker regions. The GST fusion proteins were pulled-down using glutathion-sepharose beads and co-purified PDE4 variants were detected by Western blotting. 4A4 interacts with the Lyn/SH3 domain (lanes 2 and 6) and this interaction is not impaired by nested deletion of UCR1C in the monomeric 4A4ΔUCR1C (lane 8). PDE4D does not bind to Lyn/SH3 directly (lane 4), but can be co-purified if co-expressed with 4A4 (lane 6), but not the monomeric 4A4UCR1C construct (lane 8). Western blots are representative of experiments performed three times.